Biogeochemistry (2008) 90:129–140
DOI 10.1007/s10533-008-9239-y

The Siak, a tropical black water river in central Sumatra on the verge of anoxia

Tim Rixen · Antje Baum · Thomas Pohlmann · Wolfgang Balzer · Joko Samiaji · Christine Jose

Received: 28 January 2008 / Accepted: 22 August 2008 / Published online: 16 September 2008

Abstract The Siak is a black water river in central Sumatra, Indonesia, which owes its brown color to dissolved organic matter (DOM) leached from surrounding, heavily disturbed peat soils. The dissolved organic carbon (DOC) concentrations measured during five expeditions in the Siak between 2004 and 2006 are among the highest reported world wide. The DOM decomposition appeared to be a main factor influencing the oxygen concentration in the Siak which showed values down to 12 μmol l^{-1}. Results derived from a box-diffusion model indicated that in addition to the DOC concentration and the associated DOM decomposition the water-depth also plays a crucial role in regulating the oxygen levels in the river because of its impact on the turbulence in the aquatic boundary layer and the surface/volume ratio of water in the river. Model results imply furthermore that a reduced water-depth could counteract an increased oxygen consumption caused by an enhanced DOM leaching during the transition from dry to wet periods. This buffer mechanism seems to be close to its limits as indicated by sensitivity studies which showed in line with measured data that an increase of the DOC concentrations by ~15% could already lead to anoxic conditions in the Siak. This emphasizes the sensitivity of the Siak against further peat soil degradation, which is assumed to increase DOC concentrations in the rivers.

Keywords Anoxia · Black water river · Peat · Sumatra

Abbreviations

A_V	Diffusion coefficient
C	Carbon
C_{Oxygen}	Oxygen consumption rate
C/O ratio	Ratio between organic carbon and oxygen
DOC	Dissolved organic carbon
DOM	Dissolved organic matter
ENSO	El Niño Southern Oscillation
F_{Oxygen}	Oxygen flux rate across the air–water interface
k	Piston velocity
O_2	Oxygen concentration
O_{2sat}	Oxygen saturation concentration
$[O_2]_{River}$	Oxygen concentration in the river water

T. Rixen (✉) · A. Baum
Zentrum für Marine Tropenökologie, Fahrenheitstr. 6, 28359 Bremen, Germany
e-mail: trixen@uni-bremen.de

T. Pohlmann
Zentrum für Meeres- und Klimaforschung, Institut für Meereskunde, Universität Hamburg, Bundesstr. 53, 20146 Hamburg, Germany

W. Balzer
Universität Bremen, FB2 Meereschemie (UBMCh), Postfach 330440, 28334 Bremen, Germany

J. Samiaji · C. Jose
University of Riau, Jl. Simpang Panam Km 12.5, Pekanbaru, Riau, Indonesia

pO_2	Oxygen partial pressure
$pO_{2\text{-}Atmospere}$	Partial pressure of oxygen in the atmosphere
$pO_{2\text{-}River}$	Partial pressure of oxygen in the river water
Tg	Terra gram
S_{Oxygen}	Oxygen flux through the sea surface into the surface layer
SOI	Southern Oscillation Index
S.	Sungai (river)
u_{diff}	Diffusion velocity
UV	Ultra violet
α	Solubility coefficient of oxygen
Δz	Thickness of the layers in the model

Introduction

In recent years there has been an increasing number of reports on anoxic (zero oxygen) and hypoxic (oxygen concentration <5 μmol l^{-1}) events occurring in estuaries and coastal zones (Diaz 2001; Naqvi et al. 2000; Rabalais 1999; Turner and Rabalais 1994). These events were often caused by eutrophication but there are also natural processes such as black water events that lead to anoxic and hypoxic conditions in rivers and estuaries (Hamilton et al. 1997; Howitt et al. 2007). Black water events are flood events during which an enhanced leaching of DOM from leaf litter colors the water dark brown; the subsequent decay thereof reduces the oxygen concentration in the water. Although oxygen consumption is generally considered to be the main cause of low oxygen levels in aquatic systems, the oxygen concentrations in the water are the product of a complex interplay between oxygen consumption and reaeration (Paerl 2006). This interplay has not yet been studied in black water rivers draining the Indonesian peat lands.

Indonesia holds approximately 56% of the tropical peat soil area ($\sim 20.0 \times 10^{10}$ m^2 Rieley et al. 1996) that sequestered as much organic carbon (10–30 Tg C $year^{-1}$) as the global deep sea sediments in their original state (Jahnke 1996; Sorensen 1993). Today approximately 45% of the former Indonesian peat swamp forest has been lost (Hooijer et al. 2006) and large parts of the peat lands have been converted into rubber estates and particularly palm oil estates (Angelsen 1995; Hooijer et al. 2006). Due to aerobic peat decomposition and fires kindled by common agricultural slash-and-burn practices, disturbed peat lands turned into CO_2 sources. Current estimates on CO_2 emissions from drained Indonesian peat lands are at >485 Tg C $year^{-1}$ and thus even >4 times higher than the Indonesian CO_2 emissions caused by burning fossil fuel, cement production and gas flaring (103 Tg C $year^{-1}$ in 2004 Marland et al. 2007). The dramatic destabilization of Indonesian peat lands and the resulting mobilization of carbon emphasize the need to assess the vulnerability of tropical peat-draining rivers such as the Siak in central Sumatra in the fact of associated environmental changes (Fig. 1). Therefore five expeditions to the Siak were carried out between 2004 and 2006 during which DOC, oxygen, salinity and temperature were measured along the river. Furthermore, DOM decomposition experiments were conducted and a box-diffusion model developed in order to study the oxygen dynamics in the river.

Study area and methods

Central Sumatra experiences high rainfall and a weakly pronounced seasonality with a dry season (May–September) and a rainy season (October–April) due to the meridional variation of the inter-tropical convergence zone (Fig. 2). On inter-annual time scales the precipitation rates are influenced by the climate anomaly El Niño/Southern Oscillation (ENSO, Ropelewski and Halpert 1987). During our expeditions between 2004 and 2006 ENSO forcing was moderate compared to the pronounced El Niño event in 1997/1998 in the course of which the Southern Oscillation Index (SOI) revealed values <−5. Nevertheless, weakly pronounced El Niño conditions prevailed during the dry season 2005 and 2006 whereas ENSO was in positive mode referred to as La Niña during the rainy season 2005/2006.

The Siak is one of the main peat-draining rivers in central Sumatra in which high DOM inputs caused by leaching from the surrounding peat soils reduces light penetration to depths of ~15–20 cm (Baum et al. 2007). The Siak originates at the confluence of the tributaries S. Tapung Kanan and S. Tapung Kiri (Fig. 1). It passes through the adjacent lowlands and discharges into the Malacca Strait after 370 km. The S. Tapung Kanan and the Mandau, the main tributaries of the Siak, originate in the peat swamps and

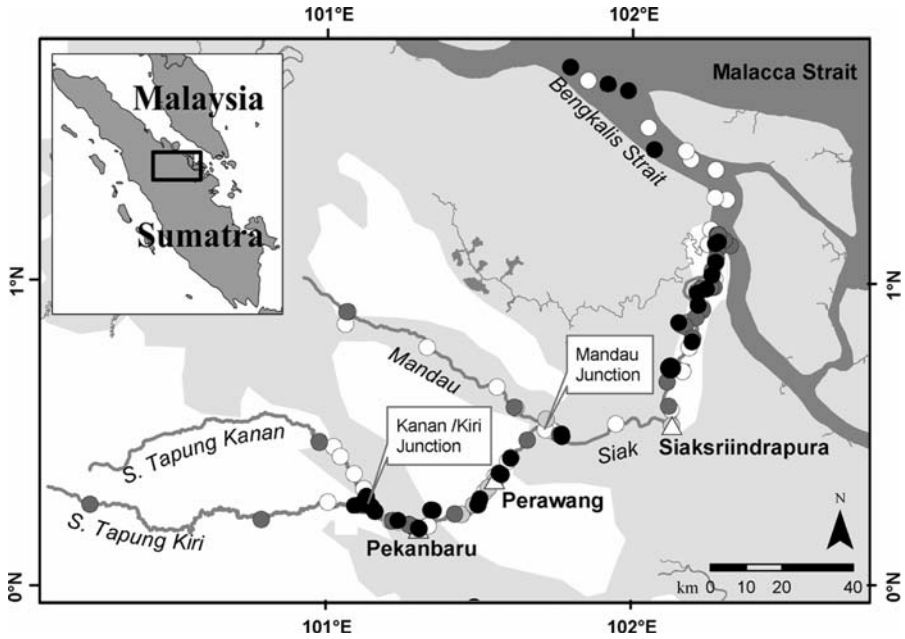

Fig. 1 Study area: The Siak with its headstreams S. Tapung Kiri and S. Tapung Kanan, and its tributary Mandau. The locations of the main cities (Pekanbaru, Perawang, and Siaksriindrapura) are indicated by triangles. Peat soil distribution (marked in grey) is obtained from the FAO (2003). Samples collected during the expedition in March and September 2004 as well as in July/August 2005 and March 2006 are indicated by the light grey, dark grey, white, and black circles, respectively. To maintain the figure as clear as possible the sampling sites during the November 2006 expedition, which are also located between Pekanbaru and the Bengkalis Strait, are not shown

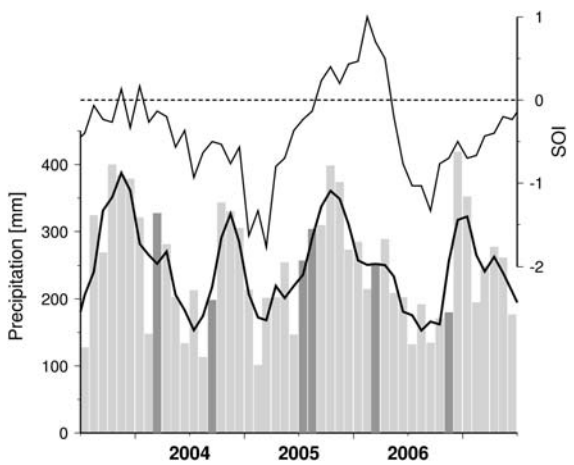

Fig. 2 Precipitation rates obtained from DWD (2006) and averaged for the area 1° S–1° N and 100–102° E are indicated by the grey bars. The dark grey bars show the months during which the expeditions were carried out. The black bold line shows the precipitation rates smoothed with a 3-month moving average. The Southern Oscillation Index (SOI) was obtained from http://www.cpc.ncep.noaa.gov/data/indices/soi) and also smoothed with a three-month moving average

join the Siak at river km 155 and 245, respectively. The Siak catchment (11,500 km^2) consists to approximately 45% of peat lands which have largely been converted into palm oil and rubber estates as well as shrub lands (Laumonier 1997).

During the five expeditions to the Siak between 2004 and 2006 (Table 1) water samples for determining DOC, dissolved oxygen and salinity were taken using a Niskin bottle at a water-depth of 1 m along the river (Figs. 1, 3). All samples were taken during the day time. DOC samples were filtered through 0.45 µm filters into pre-combusted 20 ml FIOLAX ampoules. The samples were subsequently acidified (20% phosphoric acid) to a pH value of ~2, sealed, and stored at ~4°C in darkness until they were analyzed after the expeditions. DOC was analyzed using a high temperature catalytic oxidation method (Dohrman DC-190 analyzer). Oxygen concentrations were determined using Winkler titration and salinity was measured by a WTW Tetra Con 325_3. A more detailed description of the methods applied is given by Baum et al. (2007). During the third expedition, oxygen, salinity and

Table 1 Sampling period, mean water temperatures, precipitation rates (obtained from DWD 2006, see Fig. 2), water discharges as derived from the precipitation rates (see Baum et al. (2007), for more detailed information), and DOC riverine end-member concentrations as indicated by the regression equations shown in Fig. 4a

Sampling period		Temp.	Precipit.	Discharge	DOC
Month	Year	(°C)	(mm)	(m^3 s^{-1})	(μmol l^{-1})
March	2004	29.4	327	645	1,866[a]
September	2004	30.1	199	391/99[b]	2,195
July/August	2005	29.5	304	599	2,247
March	2006	30.5	254	500	1,613
November	2006	29.7	180	355	1,793
Mean		29.8	253	498/440	1,942

[a] This riverine DOC end-member concentration was estimated based on DOC concentrations measured in the Siak upstream the estuary as no samples were taken in the estuary during the expedition in March 2004 (see Baum et al. 2007)

[b] The measured water discharge was 99 m^3 s^{-1} (see Baum et al. 2007)

temperature profiles were also obtained using a Sea-Bird SBE19plus. Due to logistical constraints the sampling campaign was restricted to the upper course of the Siak in March 2004 and oxygen concentrations could not be measured during the last expedition in November 2006.

In March 2006, a DOM microbial and photochemical degradation experiment was initiated for which water was collected a few kilometer downstream the Mandau junction (Fig. 1). The water collected was immediately filled into eight ~20 ml FIOLAX ampoules. The half-filled ampoules were sealed and exposed to sunlight until they were opened and preserved as the other DOC samples. The DOC concentrations measured in each of the incubated ampoules were plotted against the time at which the ampoules were opened (Fig. 4). Since we left the study site after 336 h (14 days), the remaining incubated sample was exposed to artificial sunlight (Ocean light 150 HQ I) until it was analyzed after 3,148 h (131 days). The UV-transmittance of the FIOLAX glass ampoules was determined using a spectrophotometer (Libra S12) with sensors for UV-A (315–400 nm) and UV-B (280–315 nm). The results showed that ~5% of the UV-A and ~38% of the UV-B irradiance were absorbed by the glass ampoules. Since the UV absorption and the artificial sunlight could have reduced the photochemical degradation, the DOM decay determined in the experiment must be considered to be an underestimate rather than an overestimate.

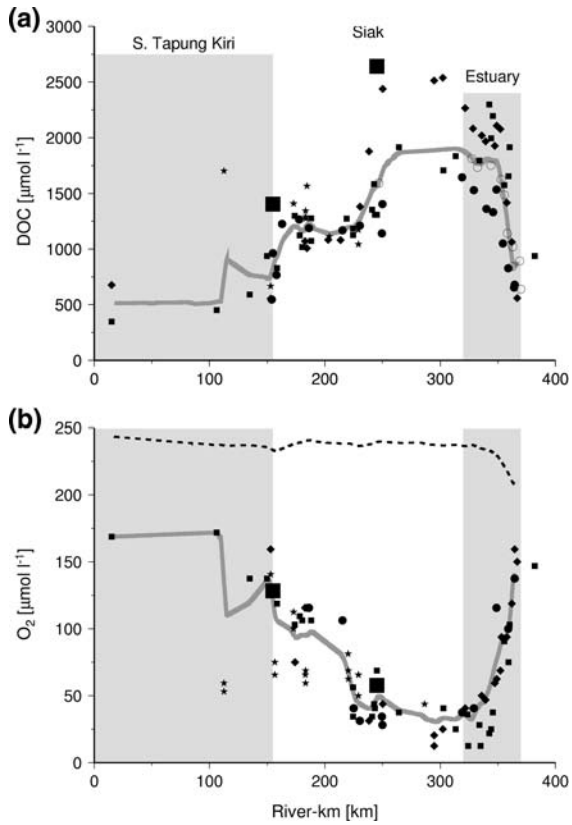

Fig. 3 DOC (**a**) and oxygen concentrations (**b**) measured at a water-depth of 1 m versus river-km. The river-km zero represents the origin of the S. Tapung Kiri in the highlands. At river-km 320 increasing salinity indicates the beginning of the estuary (salinity data are not shown) and at river-km 370 the Siak discharges into the Malacca Strait. The Kanan/Kiri and the Mandau junctions are at river-km 155 and 245. The mean oxygen and DOC concentrations in the Mandau and S. Tapung Kanan are shown by the large black squares. Data measured during the first, second, third, fourth and fifth expeditions are indicated by stars, diamonds, squares, circles and open circles. The averaged DOC and oxygen concentrations are shown by the grey lines and the broken line in '**b**' indicates the mean oxygen saturation concentrations calculated after Benson and Krause (1984)

Results and discussion

DOC concentration

The DOC concentrations in the Siak increased from approximately 500–1,300 and from 1,300 to

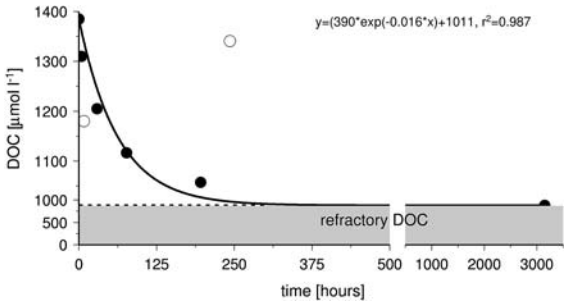

Fig. 4 DOM decomposition experiment showing decreasing DOC concentrations (circles) over time of incubation. Note that the scale of the *y*-axis changes at 1,000 µmol l^{-1}. The grey shaded area represents the part of the DOC which appears to be refractory against microbial and photochemical oxidation on the considered time scale. The plotted function describes the exponential decomposition of the degradable DOC as shown by the black line. In fitting the exponential function to the data, the two outliers as indicated by the open circles, were ignored

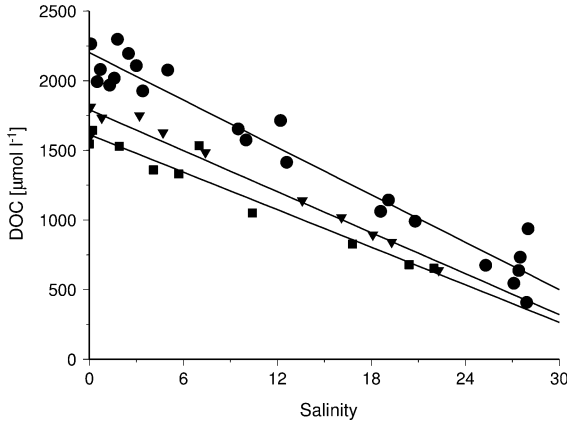

Fig. 5 DOC concentrations (circles, Sep. 2004, July/August 2005; squares, March 2006; triangles, November 2006) versus salinity. DOC concentrations at the zero intercept of the y-axis are considered as the riverine DOC end-member concentrations (see Table 1)

1,900 µmol l^{-1} around the Kanan/Kiri and Mandau junctions due to high DOM inputs from peat-draining lowland rivers S. Tapung Kanan and Mandau (Figs. 1, 3a, Baum et al. 2007). The Mandau, which is assumed to contribute half of the DOM that was carried into the Siak estuary, revealed DOC concentrations of as high as 3,600 µmol l^{-1}. According to global compilations (Harrison et al. 2005; Hope et al. 1994), such a high DOC concentration has only been exceeded by one river (the Oyster river). Rising DOC concentrations in rivers were suggested to indicate a destabilization of peat soils at higher latitudes caused by climate change (Freeman et al. 2001, 2004). In the Siak catchment peat soils are destabilized by deforestation, drainage, and conversion of peat swamp forests into palm oil and rubber estates as mentioned earlier. Accordingly, peat soil leaching and the resulting high DOC concentrations in the Siak and its tributaries can not be considered natural. On the other hand, anthropogenic enhanced leaching as seen in other studies (Holden 2005; Holden et al. 2004) is very difficult to quantify as there is no data available on the Siak prior to the main deforestations.

In the estuary, decreasing DOC concentrations correlating to increasing salinity suggested that dilution of the DOM-rich Siak water by DOM-poor ocean water was an important factor controlling the DOC concentration in the estuary (Fig. 5). The zero intercept of the *y*-axis as shown by the regression equation is often considered as riverine DOC end-member concentration (e.g., Alvarez-Salgado and Miller 1998; Mantoura and Woodward 1983; Miller 1999). DOC end-member concentrations determined for each of the five expeditions ranged from 1,613 to 2,247 with lower concentrations corresponding to the end of the rainy season (March 2004 and 2006) and during the dry season (November 2006) (Fig. 2, Table 1). Higer DOC end-member concentrations were measured at the end of the dry season (September 2004 and July/August 2005) suggesting, as also observed in other studies (Hamilton et al. 1997), that increasing precipitation rates enhance DOM leaching from soils, especially after dry periods. During the expedition in September 2004, a low ground water level still attested to the preceding dry period and the water discharge measured was significantly lower than predicted from precipitation rates (see Table 1). It was therefore assumed that the increasing precipitation rates were still filling up the soil and ground water reservoir (Baum et al. 2007).

DOM decomposition

The DOM decomposition experiment showed that in the river water collected downstream of the Mandau junction approximately 27% of the DOC ($\sim$374 µmol l^{-1}) was degradable within a 2 week period whereas 73% of the DOC appeared to be refractory on time scales of days to months (Fig. 4).

The decreasing DOC concentrations measured during the DOM decomposition experiment suggest an exponential DOM decay which can be described by the following equation:

$$\mathrm{DOC(t)} = (\mathrm{DOC}_{t0} * 0.27) * \exp(-0.016 * t) + (\mathrm{DOC}_{t0} * 0.73) \quad (1)$$

DOC(t) is the DOC concentration at a certain time (t) and DOC_{t0} is the DOC concentration at the beginning of the experiment. The resulting decay constant (λ) of $-0.016\ \mathrm{h}^{-1}$ indicates a half-life of 43 h for the most labile fraction (half-life = ln(2)/λ) and the first derivation of Eq. 1 describes the DOM decomposition rate ($\mathrm{DOM}_{\mathrm{decomposition}}$):

$$\mathrm{DOM}_{\mathrm{decomposition}} = \frac{\partial \mathrm{DOC}(t)}{\partial t} \quad (2)$$

Since peat contains a mass ratio between organic carbon and oxygen (C/O ratio) of ~2.7 (Cameron et al. 1989), it was assumed that only 0.8 mol of dissolved oxygen was consumed during oxidation of one mol of peat-derived DOC ($\mathrm{DOM} + 0.8\mathrm{O}_2 \rightarrow \mathrm{CO}_2$). Consequently the DOM decomposition rate (Eq. 2) can be converted into the oxygen consumption rate (C_{Oxygen}) by multiplying it by 0.8:

$$C_{\mathrm{Oxygen}} = 0.8 * \frac{\partial \mathrm{DOC}(t)}{\partial t} \quad (3)$$

According to Eq. 1–3, a mean DOC concentration of ~1,500 µmol l^{-1} (DOC_{t0}) as derived from the data measured in the Siak upstream the estuary (Fig. 3a), suggests, for example, a mean oxygen consumption rate of ~5.1 µmol l^{-1} h^{-1}. Such an oxygen consumption rate is ~3 times higher than those determined in the Amazon river (1.7 µmol l^{-1} h^{-1} (Devol et al. 1987) and must be considered as a minimum estimate for reasons discussed above. Furthermore, such a high DOC decomposition rate implies a net DOC degradation with the water travel time in the Siak river. The observation that the DOC concentrations increased from headwater to estuary indicates that DOC inputs exceeded the DOC decay; this imbalance was most pronounced at the Kanan/Kiri and the Mandau junctions mentioned above (Fig. 3a).

Oxygen concentrations

Oxygen concentrations decreased from ~170 µmol l^{-1} in the S. Tapung Kiri to 12 µmol l^{-1} at the beginning of the Siak estuary (Fig. 3b) and the water column had weak or no vertical gradient, as seen in the oxygen profiles obtained by the Sea-Bird19plus CTD during the expedition in July/August 2005 (Fig. 6). The oxygen concentrations were inversely correlated to the DOC concentrations suggesting that DOM decomposition was a main factor controlling the oxygen concentration in the Siak (Fig. 7). Furthermore, the regression equation and the resulting zero intercept of the x-axis, implies that anoxic conditions should be established in the Siak when the DOC reaches concentrations of ~2,850 µmol l^{-1} (= 145.48/0.051; see equation given in Fig. 7). In the Paraguay river, for example, an enhanced DOM leaching after a dry period produced an anoxic event associated with an fish kill and the DOC concentrations range from ~700 to 925 µmol l^{-1} (Hamilton et al. 1997). There are also reports of mass fish mortalities in the Siak but so far we have not been able to observe such an event.

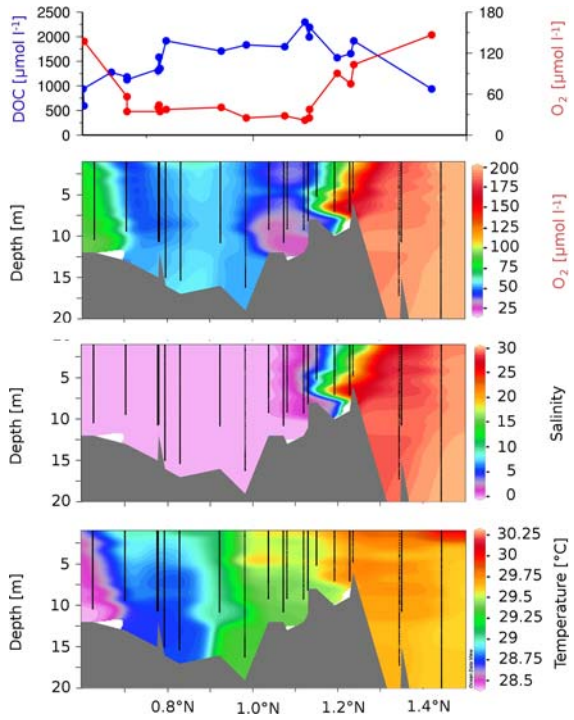

Fig. 6 DOC and oxygen concentrations measured in the Siak downstream river-km 180 at a water depth of one m (upper panel) versus latitude as well as oxygen concentrations, salinity and temperature determined with the Seabird CTD versus latitude (lower panels). In the lower panels the grey area indicates the river bed and the black lines the CTD casts

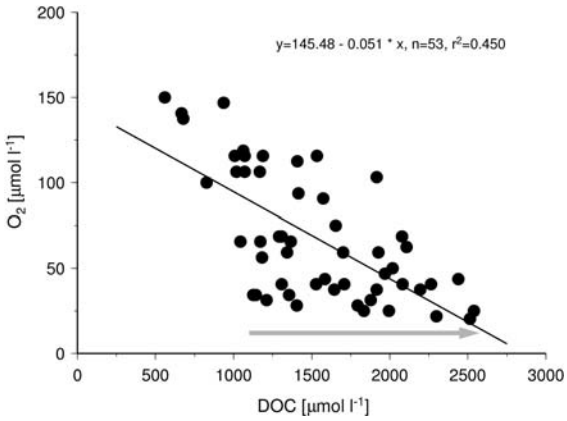

Fig. 7 Oxygen versus DOC concentrations measured at water-depth of 1 m during the expeditions. The black line illustrates the given regression equations, '*n*' is the number of data points and '*r*' is Pearson correlation coefficient. The arrow indicates the range of data over which increasing DOC concentration is not necessarily associated with reduced oxygen concentrations

Although the correlation between DOC and oxygen concentrations is statistically significant (significance level <0.1%), outliers point to other processes that counteract the influence of DOM decomposition on oxygen concentration in the Siak.

Oxygen inputs

Oxygen production during the photosynthesis of organic matter could in principle be an oxygen source which might have enhanced the oxygen concentrations in the Siak during the daytime. Since the lack of light caused by the brown water color strongly reduces photosynthesis, it is assumed that oxygen inputs across the air–water interface are the main source of oxygen in the Siak. This oxygen flux (F_{Oxygen}) is driven by the oxygen partial pressure (pO_2) difference between the river and the atmosphere and can be calculated according to Fick's law:

$$F_{\mathrm{Oxygen}} = k * \alpha\left(\mathrm{pO}_{2-\mathrm{Atmosphere}} - \mathrm{pO}_{2-\mathrm{River}}\right) \qquad (4)$$

'α' is the temperature- and salinity-dependent solubility coefficient of oxygen ($\alpha = [O_2]/pO_2$) which was calculated according to Benson and Krause (1984) and '*k*' is the piston velocity, which is mainly controlled by the turbulence in the aquatic boundary layer. The turbulence in the aquatic boundary layer strongly depends on the bottom friction and can be increased by wind speeds and precipitation rates (e.g., Borges et al. 2004; Guerin et al. 2007; Kremer et al. 2003; Raymond and Cole 2001). The bottom friction, in turn, generally increases with decreasing water-depth and increasing current velocity (Raymond and Cole 2001). Results of measurements made in the Amazon river, by determining ^{222}Rn accumulation in free-floating chambers and carrying out oxygen mass balances, indicate mean piston velocities of up to 7 and 25 cm h^{-1}, respectively (Devol et al. 1987).

Oxygen dynamics

In order to examine the interplay between oxygen consumption and oxygen input, we developed a small box-diffusion model (Eq. 5) within which the water column of the river was divided into 100 cm thick layers (Δz) and a time step of 13.5 s was considered.

$$\frac{\partial \mathrm{O}_2}{\partial t} = \frac{\partial}{\partial z}\left(A_{\mathrm{v}}\frac{\partial \mathrm{O}_2}{\partial z}\right) + S_{\mathrm{Oxygen}} + C_{\mathrm{Oxygen}} \qquad (5)$$

S_{Oxygen} is the oxygen source term in the surface layer. If in a discrete model the surface layer has a thickness Δz, the oxygen source term in this layer can be derived from the oxygen flux through the air-water surface (F_{Oxygen}, see Eq. 4) by means of: $S_{\mathrm{Oxygen}} = F_{\mathrm{Oxygen}}/\Delta z$. C_{Oxygen} (see Eq. 3) is the oxygen consumption rate in the water column and 'A_{V}' is the diffusion coefficient for which a value of 370 cm^2 s^{-1} was selected. Determination of the diffusion velocity u_{diff} by means of $u_{\mathrm{diff}} = \sqrt{2 \cdot A_{\mathrm{V}}/t}$, leads to the conclusion that due to the mean water depth of <20 m (see Fig. 6) diffusion affects the entire water column after approximately ~1.5 h. Accordingly it is inferred that a variation of the chosen A_{V} in a realistic range would also result in a rapid mixing which agrees with the well-mixed water body seen in the salinity and temperature profiles (Fig. 6). Equation 5 is formulated forward in time and as central differences in space. An explicit scheme was employed to solve this equation, which made it necessary to use the above-mentioned small time step of 13.5 s. A test of this scheme prior to our simulation proved that it fulfils all mass conservation requirements.

Water-depth and piston velocity

In order to check the applicability of the model for the Siak, we first averaged the DOC and oxygen concentrations measured just upstream from the

estuary. The resulting mean DOC concentration of 1,500 μmol l^{-1} was used to calculate the oxygen consumption (Eq. 3) and after reaching the steady state, the simulated oxygen concentration was compared to the mean measured oxygen concentrations of 59 μmol l^{-1}. The modeled oxygen concentrations varied depending on the selected piston velocity and the water-depth. As discussed previously the piston velocity strongly influences the oxygen input across the air–water interface and the water-depth affects the total oxygen consumption in the water column. The total oxygen consumption within a given time is the product of the oxygen consumption rate (see Eq. 3) and the considered water volume. Since the time step of 13.5 s and the river surface area are constant in the model, the total oxygen consumption increases with an increasing water-depth. One therefore has to increase the piston velocities as water-depth increases in order to maintain an oxygen concentration of 59 μmol l^{-1} in the modeled water column (Fig. 8). A piston velocity of 22.9 cm h^{-1} would, for example, correspond with a water-depth of 8 m, in order to simulate a mean oxygen concentration of 59 μmol l^{-1} (Fig. 9, see also Table 2—experiment 1). Such a mean water-depth appears to be representative for the Siak considering that the water-depth at our sampling sites ranged between ~8 and 20 m (see Fig. 6) and the sites were located near the centre and not close to the river banks.

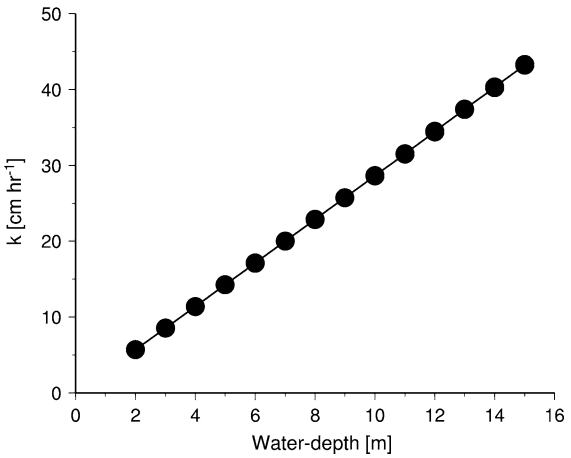

Fig. 8 Piston velocities (k) versus water-depth. Each data point indicates a model result. In each model run a DOC concentration of 1,500 μmol l^{-1} was considered, and to each given water-depth a piston velocity was selected in a way that the oxygen concentration at steady state was maintained at 59 μmol l^{-1}

Since a piston velocity of 22.9 cm h^{-1} is also close to the one derived form the oxygen mass balance calculation in the Amazon (Devol et al. 1987), it can be concluded that the model is suitable to study the oxygen dynamics in the Siak river.

Residence time and current velocities

As indicated by the previous model run (see Fig. 9) it takes up to 120 h (5 days) to reach a steady state in the dissolved oxygen concentrations so that residence time of water in the Siak and thus the current velocity could be an important factor influencing the oxygen concentration in the river. In order to study the possible impact of the current velocity on the oxygen concentration we chose a piston velocity of 25 cm h^{-1} and a mean water-depth of 8 m and plotted the modeled oxygen concentrations versus 'river-km' (Fig. 10a). River-km was calculated by multiplying the time-step of 13.5 s and current velocity. The product was kept constant by reducing the number of time-steps in the simulation when the current velocity was increased. Furthermore, the initial DOC concentration was set at 520 μmol l^{-1} as measured in the S. Tapung Kiri (see Fig. 3a) and was subsequently increased on a step by step basis at river-km 105 and 215 to 1,300 and 1,900 μmol l^{-1} in order to simulate DOM inputs from the S. Tapung Kanan and Mandau. The selected river-km's are actually ~30–50 km upstream of the Kanan/Kiri and Mandau junction at river km 155 and 245. The shift reflects the tidal influence at the Mandau junction and DOM inputs of smaller peat draining creeks into to the S. Tapung Kiri already prior to the Kanan/Kiri junctions. However, a selected mean current velocity of 1 m s^{-1} results in oxygen concentrations which are higher than those measured because of the short residence time (~2.4 days) and a resulting lower DOM consumption in the river (Fig. 10a, Table 2—experiment 2). If one selects mean current velocities (residence times) of 0.25 m s^{-1} (~9.8 days) and 0.125 m s^{-1} (~18 days), the resulting oxygen concentrations correspond reasonably well with the measured oxygen concentrations in the Siak (Fig. 10a, Table 2—experiments 4 and 5). Direct determination of mean current velocities in tidal-influenced rivers is very problematic but can be deduced from the mean water discharge and the mean river cross section. A mean water discharge of 440 m^3 s^{-1} (Table 1), a mean water-depth of 8 m as

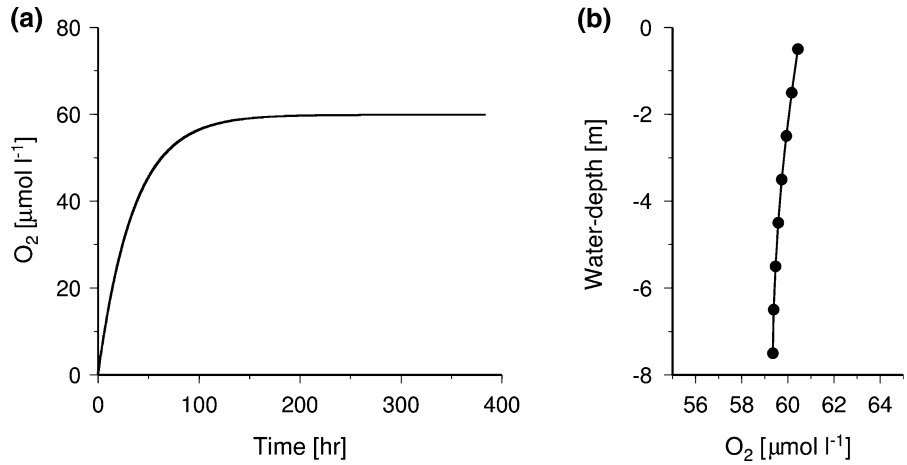

Fig. 9 Oxygen concentrations derived from the model versus time (**a**) and depicted as vertical variation in concentration at steady state (**b**; see Table 2 experiment 1)

Table 2 Result of model simulation, showing experiment number, topic of the experiment, DOC concentrations used in the model runs, modeled oxygen concentrations at the beginning of the estuary (see Figs. 10, 12), and the associated oxygen consumption rates as well as the piston velocity (k), current velocity, water-depth, and temperatures during the model experiments

Experiment no.	Topic	DOC (µmol l^{-1})	O_2 (µmol l^{-1})	O_2-cons. (µmol l^{-1} h^{-1})	k (cm h^{-1})	Velocity (m s^{-1})	Water-depth (m)	Temperature (°C)
1	Average	1,500	59	5.18	22.9		8	29
2	Velocity	1,900	67	6.56	25.0	1.000	8	29
3	Velocity	1,900	41	6.56	25.0	0.500	8	29
4	Velocity	1,900	32	6.56	25.0	0.250	8	29
5	Velocity	1,900	31	6.56	25.0	0.125	8	29
6	Temperature	1,900	28	6.56	25.0	0.250	8	30
7	Water-depth	1,900	58	6.56	25.0	0.250	7	29
8	DOC	2,185	1	7.55	25.0	0.250	8	29
9	Low ground	2,550	22	8.80	28.1	0.250	7	29
10	l.g. DOC	2,932	0	10.10	28.1	0.250	7	29

'low ground' and 'l.g.' means low groundwater levels

indicated by the model results and a river-width of 220 m would, for example, suggest a mean current velocity of $\sim$0.25 m s^{-1}. Since the Siak already reveals a width of 80 m at the Kanan/Kiri junction which increases to 250 m at the Mandau junction and to >350 m at the beginning of the estuary, a mean river-width of >220 m and therefore also a mean current velocity of <0.25 m s^{-1} would appear to be acceptable.

Sensitivity experiment

Temperature, water-depth, DOC

Sensitivity experiment were carried out in order to investigate the impact of possible environmental changes on the oxygen concentration in the Siak. We therefore increased the temperature and reduced the water-depth in the model because of changes in precipitation rates and the river discharge as observed, e.g., during the expedition in September 2004 (Fig. 10b). DOC concentrations were also increased due to a possible anthropogenically enhanced DOM leaching.

Temperature changes affect the oxygen input across the air–water interface by their impact on the solubility of oxygen in the water (see Eq. 4, Benson and Krause 1984). In the model a temperature increase of 1°C would lower the oxygen concentrations by $\sim$4 µmol l^{-1}. A reduction of the water-depth would increase the oxygen concentrations by $\sim$26 µmol l^{-1} (Fig. 10b, Table 2—experiments 6

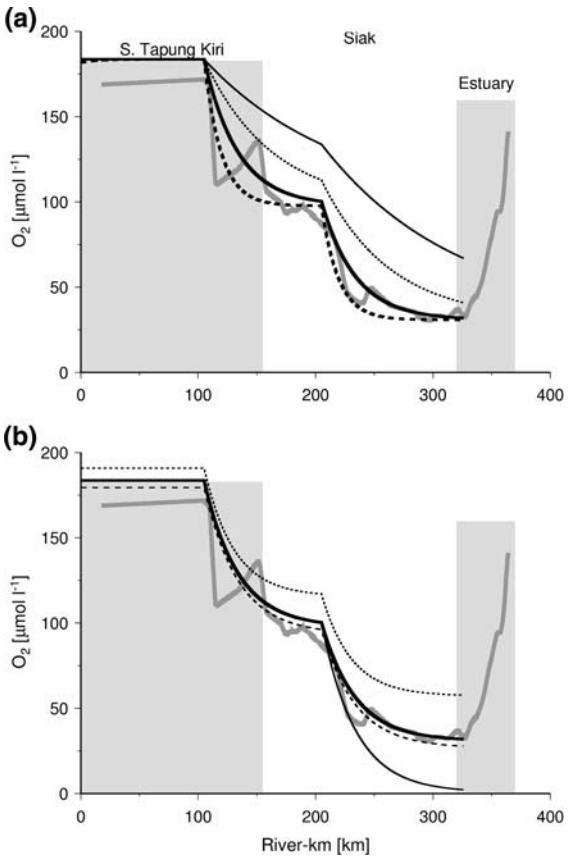

Fig. 10 (**a**) Oxygen concentrations calculated by using a mean current velocity of 1 (black line), 0.5 (dotted line), 0.25 (bold line), and 0.125 m s^{-1} (bold broken line) versus river-km (see Table 2 experiments 2–5). (**b**) Oxygen concentrations calculated by using a current velocity of 0.25 m s^{-1} (bold line, Table 2—experiment 4). The same current velocity was used also by the other model runs during which the temperature was increased by 1°C (stippled line, Table 2—experiment 6), the water-depth was decreased by 1 m (dotted line, Table 2 experiment 7) and the DOC concentration was increased by 15% (thin black line, Table 2—experiment 8). The bold grey indicated the mean measured oxygen concentrations as shown in Fig. 3b

and 7) because it would lower the total oxygen consumption in the water column as discussed above. An increase of the DOC concentration by 15% below the Mandau junction would already suffice to produce anoxic conditions in the Siak upstream the estuary (Table 2—experiment 8).

Enhanced DOC concentrations at the end of dry period

Increasing the mean DOC concentration by 15% would result in a DOC concentration of 2,185 µmol l^{-1} between the Mandau junction and the estuary. This concentration falls below DOC concentrations of ~2,550 µmol l^{-1} measured in this area e.g., during the expedition in September 2004 (Fig. 3a). Although these high measured DOC concentrations were associated with low oxygen concentrations, the latter still varied around 20 µmol l^{-1} and were not zero as indicated by the sensitivity experiment (Figs. 3b, 7). As also mentioned previously, the groundwater level was extremely low during this expedition due to dry conditions prior to the expedition. In addition to a decrease of the total oxygen consumption, a low ground water level and the resulting reduced water-depth could also enhance the turbulence in the aquatic boundary layer and thus the piston velocity and the oxygen flux across the air–water interface. We carried out further sensitivity experiments in order to test to what extent a reduced water-depth could counteract an enhanced oxygen consumption rate caused by an increase in the DOC concentration. Within these experiments the DOC concentration was set to 2,550 µmol l^{-1} after the Mandau junction and the water-depth was reduced by up to 5 m (Fig. 11). The model results indicated that a drop in the water-depth of 2 m would suffice to explain an oxygen concentration of >20 µmol l^{-1} even if the DOC concentration reached 2,550 µmol l^{-1}. If one also assumes that the piston velocity increases by 12% when the water-depth decreases by one meter (~12%), a reduction of the water-depth by 1 m could explain the data measured during the expedition in September 2004 (Figs. 11, 12, Table 2—experiment 9).

To test the sensitivity of this system to an enhanced DOC leaching the DOC concentrations were again increased by 15% to 2,932 µmol l^{-1}. According to the model results such a DOC increase would again be sufficient to produce anoxic conditions upstream of the estuary (Fig. 12, Table 2—experiment 10). The DOC concentrations of 2,932 µmol l^{-1} applied correspond fairly well with the zero intercept of the *x*-axis (~2,852 µmol l^{-1}) derived from the regression equation obtained by the correlation between the measured DOC and oxygen concentrations (Fig. 7). It is therefore assumed that water-depth is an important factor which could counteract an enhanced DOC leaching and the resulting increased oxygen consumption rates, but this buffer capacity seems to be close to its limits in the Siak.

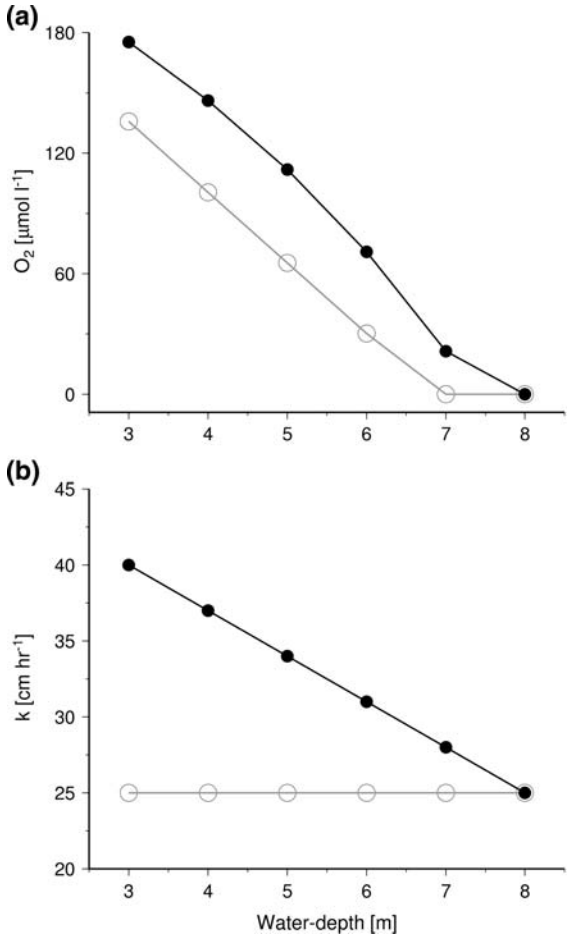

Fig. 11 Modeled oxygen concentrations at the beginning of the estuary (**a**) and the selected piston velocity (**b**) versus water-depth used in the model runs. The open circles show oxygen concentrations which result from the constant piston velocity of 25 cm h^{-1} as shown in **b**. The black circles indicate the oxygen concentrations which results from model runs in which the water-depth and the piston velocity were changed

Conclusion

Our results showed that the DOC concentrations increase along the Siak river because DOM inputs exceed DOM decay. DOM decomposition and the resulting oxygen consumption fueled by continuous DOM inputs appeared to be a main factor influencing the oxygen concentration in the Siak. This result could be confirmed by a box-diffusion model which showed that in addition to the DOC concentration the water-depth is also an important factor influencing the oxygen concentrations. The water-depth affects the oxygen input across the air water interface and the

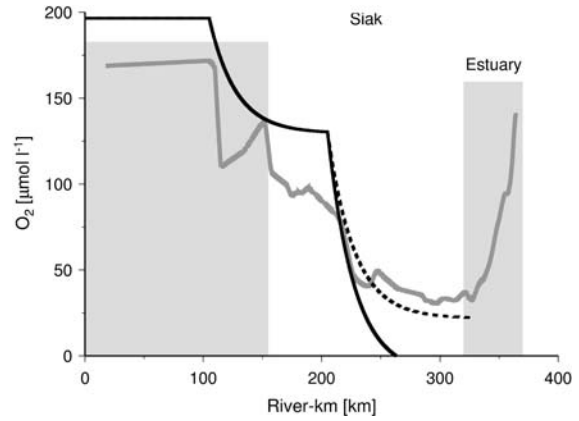

Fig. 12 Oxygen concentrations versus river-km. Oxygen concentrations calculated by using a water-depth of 7 m and a piston velocity of 28.1 cm h^{-1} are indicated by the broken black line (Table 2—experiment 9). The impact of an increase of the DOC concentrations by 15% is indicated by the black line (Table 2—experiment 10). The bold grey line indicated the mean measured oxygen concentrations as shown in Fig. 3b

total oxygen consumption in the water column due to its impact on the turbulence in the aquatic boundary layer and the surface/volume ratio of water in the river. A reduced water-depth could, for example, compensate for an enhanced oxygen consumption caused by an increased DOM leaching from soils during the transition from dry to wet periods. This result was confirmed by a box-diffusion model which suggests that buffer mechanism is close to its limit and emphasizes the sensitivity of the Siak against further peat soil degradation.

Acknowledgments We would like to thank all scientists and students from the University of Pekanbaru who helped us during our field work, the rector of the University of Riau, the captain of the research vessel R/V Senangin and his crew for their support. For helpful discussion we would like to thank the anonymous reviewer, V. Ittekkot, P. Damm our colleagues from the ZMT and Rena Kerr. We are also grateful to the Federal German Ministry for Education, Science, Research and Technology (BMBF, Bonn grant number 03F0392C-ZMT) for financial support and to R. Schlitzer as well as to P. Wessels and W.·H. F. Smith for providing Ocean Data View (ODV) and the generic mapping tools (GMT).

References

Alvarez-Salgado XA, Miller AEJ (1998) Dissolved organic carbon in a large macrotidal estuary (the Humber, U.K.): behaviour during estuarine mixing. Mar Pollut Bull 37:216–224. doi:10.1016/S0025-326X(98)00156-8

Angelsen A (1995) Shifting cultivation and "deforestation": a study from Indonesia. World Dev 23:1713–1729. doi:10.1016/0305-750X(95)00070-S

Baum A, Rixen T, Samiaji J (2007) Relevance of peat draining rivers in central Sumatra for the riverine input of dissolved organic carbon into the ocean. Estuar Coast Shelf Sci 73:563–570. doi:10.1016/j.ecss.2007.02.012

Benson BB, Krause D Jr (1984) The concentration and isotopic fractionation of oxygen dissolved in freshwater and seawater in equilibrium with the atmosphere. Limnol Oceanogr 29:620–632

Borges AV, Delille B, Schiettecatte L-S, Gazeau F, Abril G, Frankignoulle M (2004) Gas transfer velocities of CO_2 in three European estuaries (Randers Fjord, Scheldt, and Thames). Limnol Oceanogr 49:1630–1641

Cameron C, Esterle JS, Palmer CA (1989) The geology, botany and chemistry of selected peat-forming environments from temperate and tropical latitudes. Int J Coal Geol 12:105–156. doi:10.1016/0166-5162(89)90049-9

Devol AH, Quay PD, Richey JE, Martinelli LA (1987) The role of gas exchange in the inorganic carbon, oxygen, and 222Rn budgets of the Amazon River. Limnol Oceanogr 32:235–248

Diaz RJ (2001) Overview of hypoxia around the world. J Environ Qual 30:275–281

DWD (2006) Monthly precipitation (monitoring) product (1.0° gridcells). Global Precipitation Climatology Centre, Deutscher Wetterdienst, Offenbach am Main

FAO (2003) Soil map of the world. (p 1:5000000). FAO/UNESCO, Rome

Freeman C, Evans CD, Monteith DT, Reynolds B, Fenner N (2001) Export of organic carbon from peat soils. Nature 412:785. doi:10.1038/35090628

Freeman C, Fenner N, Ostle NJ, Kang H, Dowrick DJ, Reynolds B et al (2004) Export of dissolved organic carbon from peatlands under elevated carbon dioxide levels. Nature 430:195–198. doi:10.1038/nature02707

Guerin F, Abril G, Serca D, Delon C, Richard S, Delmas R et al (2007) Gas transfer velocities of CO_2 and CH_4 in a tropical reservoir and its river downstream. J Mar Syst 66:161–172. doi:10.1016/j.jmarsys.2006.03.019

Hamilton SK, Sippel SJ, Calheiros DF, Melack JM (1997) An anoxic event and other biogeochemical effects of the Pantanal wetland on the Paraguay River. Limnol Oceanogr 42:257–272

Harrison JA, Caraco N, Seitzinger S (2005) Global patterns and sources of dissolved organic matter export to the coastal zone: Results from a spatially explicit, global model. Global Biogeochem Cycles 19:GB4S04. doi:10.1029/2005GB002480

Holden J (2005) Peat land hydrology and carbon release: why small-scale process matters. Philos Trans R Soc 363:2891–2913. doi:10.1098/rsta.2005.1671

Holden J, Chapman PJ, Labadz JC (2004) Artificial drainage of peat lands: hydrological and hydrochemical process and wetland restoration. Prog Phys Geogr 28:95–123. doi:10.1191/0309133304pp403ra

Hooijer A, Silvius M, Wösten H, Page SE (2006) Peat-CO_2, assessment of CO_2 emissions from drained peat lands in SE Asia. Delft Hydraulic report Q3943. WL Delft Hydraulics, Delft, p 36

Hope D, Billett MF, Cresser MS (1994) A review of the export of carbon in river water: fluxes and processes. Environ Pollut 84:301–324. doi:10.1016/0269-7491(94)90142-2

Howitt JA, Baldwin DS, Rees GN, Williams JL (2007) Modeling black water: predicting water quality during flooding of lowland river forests. Ecol Modell 203:229–242. doi:10.1016/j.ecolmodel.2006.11.017

Jahnke RA (1996) The global ocean flux of particulate organic carbon: areal distribution and magnitude. Global Biogeochem Cycles 10:71–88. doi:10.1029/95GB03525

Kremer J, Reischauer A, D'Avanzo C (2003) Estuary-specific variation in the air-water gas exchange coefficient for oxygen. Estuaries Coasts 26:829–836

Laumonier Y (1997) The vegetation and physiography of Sumatra. Kluwer Academic Publishers, Dordrecht

Mantoura RFC, Woodward EMS (1983) Conservative behavior of riverine dissolved organic carbon in the Severn Estuary: chemical and geochemical implications. Geochim Cosmochim Acta 47:1293–1309

Marland G, Boden T, Andres RJ (2007) National CO_2 emissions from fossil-fuel burning, cement manufacture, and gas flaring: 1751–2004. Oak Ridge National Laboratory Oak Ridge, Tennessee 37831–6335

Miller AEJ (1999) Seasonal investigations of dissolved organic carbon dynamics in the Tamar Estuary, U.K. Estuar Coast Shelf Sci 49:891–908. doi:10.1006/ecss.1999.0552

Naqvi SWA, Jayakumar DA, Narvekar PV, Naik H, Sarma VVSS, D'Souza W et al (2000) Increased marine production of N_2O due to intensifying anoxia on the Indian continental shelf. Nature 408:346–349. doi:10.1038/35042551

Paerl HW (2006) Assessing and managing nutrient-enhanced eutrophication in estuarine and coastal waters: Interactive effects of human and climatic perturbations. Ecol Eng 26:40–54. doi:10.1016/j.ecoleng.2005.09.006

Rabalais NN (1999) Changes in Mississippi river nutrient fluxes and consequences for the northern Gulf of Mexico coastal ecosystem. LOIZ Newsl 13:1–3

Raymond PA, Cole JJ (2001) Gas exchange in rivers and estuaries: choosing a gas transfer velocity. Estuaries 24:312–317. doi:10.2307/1352954

Rieley JO, Ahmad-Shah AA, Brady MA (1996) The extent and nature of tropical peat swamps. In: Maltby E, Immirzi CP, Safford RJ (eds) Tropical lowland peatlands of Southeast Asia. IUCN, Gland, pp 17–53

Ropelewski CF, Halpert MS (1987) Global and regional scale precipitation patterns associated with El Nino/Southern Oscillation. Mon Weather Rev 115:1606–1626. doi:10.1175/1520-0493(1987)115<1606:GARSPP>2.0.CO;2

Sorensen KW (1993) Indonesian peat swamp forests and their role as a carbon sink. Chemosphere 27:1065–1082. doi:10.1016/0045-6535(93)90068-G

Turner RE, Rabalais NN (1994) Coastal eutrophication near the Mississippi river delta. Nature 368:619–621. doi:10.1038/368619a0